Published in final edited form as:
J Immunother. 2012 November ; 35(9): 689–701. doi:10.1097/CJI.0b013e318270dec7.

Phenotypic and Functional Attributes of Lentivirus Modified CD19-specific Human CD8+ Central Memory T Cells Manufactured at Clinical Scale

Xiuli Wang[*,1], **Araceli Naranjo**[*,1], **Christine E. Brown**[1], **Cherrilyn Bautista**[1], **ChingLam W. Wong**[1], **Wen-Chung Chang**[1], **Brenda Aguilar**[1], **Julie R. Ostberg**[1], **Stanley R. Riddell**[2,3], **Stephen J. Forman**[1], and **Michael C. Jensen**[1,2,4]

[1]Departments of Cancer Immunotherapeutics & Tumor Immunology, and Hematology and Hematopoietic Cell Transplantation, Beckman Research Institute, City of Hope National Medical Center, Duarte, CA 91010 USA

[2]Program in Immunology, Fred Hutchinson Cancer Research Center, Seattle, WA 98109 USA

[3]Institute for Advanced Studies, Technical University of Munich, Munich, Germany

[4]Center for Childhood Cancer Research, Seattle Children's Research Institute, Seattle, WA 98195 USA

Abstract

A key determinant of the therapeutic potency of adoptive T cell transfer is the extent to which infused cells can persist and expand in vivo. Ex vivo propagated virus-specific and chimeric antigen receptor (CAR) redirected anti-tumor $CD8^+$ effector T cells derived from $CD45RA^-CD62L^+$ central memory (T_{CM}) precursors engraft long-term and reconstitute functional memory following adoptive transfer. Here, we describe a clinical-scale, closed system, immunomagnetic selection method to isolate $CD8^+$ T_{CM} from peripheral blood mononuclear cells (PBMC). This method uses the CliniMACS™ device to first deplete $CD14^+$, $CD45RA^+$ and $CD4^+$ cells from PBMC, and then to positively select $CD62L^+$ cells. The average purity and yield of $CD8^+CD45RA^-CD62L^+$ T_{CM} obtained in full-scale qualification runs were 70% and 0.4% (of input PBMC), respectively. These $CD8^+$ T_{CM} are responsive to anti-CD3/CD28 bead stimulation, and can be efficiently transduced with CAR encoding lentiviral vectors, and undergo sustained expansion in IL-2/IL-15 over 3–6 weeks. The resulting $CD8^+$ T_{CM}-derived effectors ($T_{E(CM)}$) are polyclonal, retain expression of CD62L and CD28, exhibit CAR redirected anti-tumor effector function, and are capable of huIL-15-dependent in vivo homeostatic engraftment after transfer to immunodeficient NSG mice. Adoptive atherapy using purified T_{CM} cells are now the subject of an FDA authorized clinical trial for the treatment of $CD19^+$ B-cell malignancies, and three clinical cell products expressing a CD19-specific CAR for IND #14645 have already been successfully generated from lymphoma patients using this manufacturing platform.

Corresponding Author: M.C.J., Center for Childhood Cancer Research, 1100 Olive Way, Seattle, WA 98101 USA; phone: 206-987-1241; FAX: 206-884-1016; michael.jensen@seattlechildrens.org.
*Contributed equally to this work

Financial Disclosure: MCJ is an inventor of licensed patents and equity holder in ZetaRx, Inc., a licensee of these patents. All other authors have no conflicts of interest to disclose.

Keywords

T Cell Immunotherapy; Chimeric Antigen Receptor; Cell Product Manufacturing

Introduction

Adoptive T cell therapy for human malignancy has proven to be more challenging and less effective than for viral diseases. Tumor antigens that are recognized by T cells have been identified and can originate from the processing of normal tissue-specific proteins, over-expressed proteins, onco-fetal antigens, mutated proteins, or minor histocompatibility antigens (i.e., in the setting of allogeneic hematopoietic stem cell transplantation (HSCT)) (reviewed in [1]). However, isolating and expanding high-affinity tumor-specific T cells for therapy from tumor-bearing patients or healthy donors is technically difficult, and, even when successful, these T cells often fail to eliminate tumors in vivo after adoptive transfer. Important insights into the obstacles for successful tumor therapy have been derived from animal models and clinical trials. Because many tumor antigens are self-proteins that are expressed in some normal tissues, tolerance mechanisms play a role in shaping the frequency, avidity, and function of tumor-reactive T cells. Additionally, tumors evade immune recognition through a variety of mechanisms including local recruitment of regulatory T cells or other suppressor cells, loss of antigen expression, down-regulation of HLA and costimulatory molecules, and expression or secretion of inhibitory molecules or cytokines (reviewed in [2]). Finally, and perhaps most importantly, cultured tumor-reactive T cells have persisted poorly in vivo after adoptive transfer in the majority of clinical trials, even if IL-2 was administered to patients after T cell infusion [3–5].

The genetic manipulation of T cells to express introduced T cell antigen receptors or chimeric antigen receptors (CAR) makes it feasible to redirect the effector function of any type of T cell to tumors [6,7]. Consequently, there is growing interest in defining which T cell subset(s) are best suited for use in adoptive therapy and prospectively formulate cell products enriched for these subset(s). Our group has focused on identifying T cell subsets that retain the ability to persist in vivo despite their differentiation to effector cells as a consequence of in vitro activation and propagation. In nonhuman primate and NSG mouse-human T cell transfer studies we discovered a surprising dichotomy in the fate of $CD8^+$ effector T cells derived originally purified effector memory (T_{EM}) or central memory (T_{CM}) T cell precursors [8,9]. Whereas effector cells from T_{EM} ($T_{E/EM}$) rapidly undergo apoptosis following adoptive transfer and do not persist beyond 7–14 days, a subset of transferred $CD8^+$ $T_{E/CM}$ reacquired memory cell markers, reoccupied memory niches and persisted for years as functional T_{CM} and T_{EM}. These data have provided the rationale to develop a clinically useful $CD8^+$ T_{CM} purification, transduction, and expansion platform for adoptive therapy.

Here we describe a manufacturing process that incorporates clinical scale polyclonal $CD8^+$ T_{CM} isolation from leukapheresis products, T cell activation using anti-CD3/CD28 beads, lentiviral transduction, and cell expansion in IL-2/IL-15. This process uses clinical grade materials, is performed with minimal open processing steps, and reproducibly yields cryopreserved cell products in excess of 10^9 cells within 35 days. Moreover, the growth kinetics of $CD8^+$ T_{CM} are such that cultures require only the initial anti-CD3/CD28 stimulation and no exogenous feeder cells. Analysis of cell products manufactured at clinical scale using this platform reveals that T_{CM}-derived effector T cells ($T_{E/CM}$) with demonstrable CD19-specific CAR-mediated anti-tumor reactivity are reliably generated. Furthermore, significant proportions of these cells retain or reacquire phenotypic and functional attributes of T_{CM} during their in vitro culture, in particular their capacity to

persist following adoptive transfer. Our initial application of this $T_{E/CM}$ manufacturing process, which is now the subject of an FDA-authorized IND, will be to generate autologous polyclonal CAR redirected CD19-specific $CD8^+$ $T_{E/CM}$ for adoptive transfer shortly following autologous HSCT for high-risk $CD19^+$ non-Hodgkin lymphomas.

Materials and Methods

Antibodies and Flow Cytometry

Human peripheral blood mononuclear cells (PBMC) and T cells were analyzed by flow cytometry after staining with fluorochrome-conjugated monoclonal antibodies (mAbs) to CD3, CD4, CD8, CD14, CD27, CD28, CD45RA, CD45RO, CD62L, CD127 (IL7Rα) (BD Biosciences), PD1 (eBiosciences) and/or CCR7 (R&D Systems); or with Biotin-SP-conjugated Donkey anti-human Fcγ (Jackson ImmunoResearch Laboratories) and PE-conjugated streptavidin (BD Biosciences). The IOTest®Beta Mark TCR V beta Repertoire Kit (representing ~70% of normal TCR Vβ repertoire) was obtained from Beckman Coulter. Isotype-matched mAbs served as controls. Data acquisition was performed on a FACScalibur (BD Biosciences) using FCS Express V3 Software (De Novo Software).

DNA constructs and third generation self inactivating lentivirus vector

The CD19-specific scFvFc:ζ chimeric immunoreceptor, designated CD19R, has been previously described [10]. The CD19R DNA sequence (optimized by GeneArt) was cloned into a self-inactivating (SIN) lentiviral vector pHIV7 (gift from Jiing-Kuan Yee, City of Hope National Medical Center (COHNMC)) that had its CMV promoter replaced with the EF-1 promoter, and the resulting clinical grade CD19Rop-epHIV7 lentivirus was produced at the COHNMC Center for Biomedicine and Genetics (CBG) per FDA Masterfile BB-MF 9778. Using the recipient cell line HT-1080 (ATCC) for transduction, and flow cytometric analysis for human Fcγ as a read-out, the titer of the clinical preparation of CD19Rop-epHIV7 was found to be 6.3×10^7 TU/mL.

CliniMACS™ immunomagnetic $CD8^+$ T_{CM} enrichment

Leukapheresis products were obtained from consented research participants (healthy donors and lymphoma patients) under protocols approved by the COHNMC Internal Review Board. On the day of leukapheresis, PBMC were isolated by density gradient centrifugation over Ficoll-Paque (GE Healthcare) followed by two washes in PBS/EDTA. PBMC were then washed once in PBS, resuspended in X Vivo15 media (Bio Whittaker) containing 10% fetal calf serum (FCS) (Hyclone), transferred to a 300 cc transfer bag, and stored on a 3-D rotator overnight at room temperature (RT). The following day, up to 5×10^9 PBMC were incubated in a 300 cc transfer bag with clinical grade anti-CD4 (2.5 mL), anti-CD14 (1.25 mL), and anti-CD45RA (2.5 mL) microbeads (Miltenyi Biotec) for 30 minutes at RT in X Vivo15 containing 10% FCS. $CD4^+$, $CD14^+$ and $CD45RA^+$ cells were then immediately depleted using the CliniMACS™ depletion mode according to the manufacturer's instructions (Miltenyi Biotec). After centrifugation, the unlabeled negative fraction of cells was resuspended in CliniMACS™ PBS/EDTA buffer (Miltenyi Biotec) containing 0.5% human serum albumin (HSA) (CSL Behring) and then labeled with clinical grade biotinylated-DREG56 mAb (COHNMC CBG) at $0.1\mu g/10^6$ cells for 30 minutes at RT. The cells were then washed and resuspended in a final volume of 100 mL CliniMACS™ PBS/EDTA containing 0.5% HSA and transferred into a new 300 cc transfer bag. After 30 minutes incubation with 1.25 mL anti-biotin microbeads (Miltenyi Biotec), the $CD62L^+$ fraction of PBMC ($CD8^+$ T_{CM}) was purified with positive selection on CliniMACS™ according to the manufacturer's instructions, and resuspended in X Vivo15 containing 10% FCS.

Activation, lentiviral transduction and expansion of enriched CD8$^+$ T_{CM}

Within 2 hours of completing the immunomagnetic enrichment, CD8$^+$ T_{CM} were stimulated in a vented T-25 flask (Falcon) with GMP Dynabeads® Human T expander CD3/CD28 (Invitrogen) at a 1:3 ratio (T cell:bead) in 25 mL X Vivo15 containing 10% FCS, then cultured in the presence of 50 U/mL rhIL-2 (Chiron) and 0.5 ng/ml rhIL-15 (CellGenix). After a three day incubation, 5–17×10^6 cells were transduced with clinical grade CD19Rop-epHIV7 at MOIs ranging from 0 to 2.9 in 5.5 mL X Vivo15 containing 10% FCS with 5μg/mL protamine sulfate (APP Pharmaceutical), 50 U/mL rhIL-2 and 0.5 ng/mL rhIL-15 in a 32 Vuelife tissue culture bag (AFC). The bag was centrifuged for 30 minutes at 567×g at 32°C ± 3°C. After spinoculation, the bag was placed at a horizontal position on a culture rack at 37°C, 5% CO_2. Cultures were then maintained with addition of X-Vivo15 10% FCS as required to keep cell density between 3×10^5 and 2×10^6 viable cells/mL, with cytokine supplementation (final concentration of 50 U/mL rhIL-2 and 0.5 ng/mL rhIL-15) every Monday, Wednesday and Friday of culture. Based on culture volume, T cells were transferred to 730 Vuelife bags (AFC). Fourteen days or more after the lentiviral transduction, the CD3/CD28 Dynabeads were removed using the Dynal ClinEx Vivo Magnetic Particle Concentrator bag magnet, and bead-free T cells were drained into a new 730 Vuelife bag. Cultures were propagated until total cell numbers of approximately 3×10^9 cells were generated as determined by Guava PCA, at which time cultures were harvested, washed in Isolyte (Braun), then resuspended in Cryostor CS5 (BioLife Solutions) at approximately 3×10^7 cells/mL for cryopreservation using a Mr. Frosty (Nalgene) and a portable controlled rate freezer system (Custom Biogenics). In some cases, to increase cell purity, the harvested cells were washed an additional two times in Isolyte immediately prior to cryopreservation.

Supporting cell lines

Generation of EBV-transformed lymphoblastoid cell lines (LCL), LCL that express a membrane tethered CD3 epsilon specific scFv agonist OKT3 (LCL-OKT3) and NS0 cells that express human IL-15 (NS0-IL15) have been previously described[9,11]. SupB15 and K562 were obtained from the American Tissue Culture Collection (ATCC).

Western blot

Western blot analysis for CAR expression has been described previously [12]. In brief, reduced whole-cell lysates are subjected to Western blot analysis and probed with an anti-human CD3-ζ (cytoplasmic tail)-specific mAb 8D3 (BD Pharmingen). This probe detects both the 16-kDa endogenous ζ and the 66-kDa CAR ζ.

Cytotoxicity Assays

4-hour ^{51}Cr release assays were performed as previously described [13] using the indicated effector cells and ^{51}Cr-labeled target cells.

Cytokine Production Assays

Freshly thawed T cell products (10^5) were co-cultured overnight in 96-well tissue culture plates with 10^5 of the indicated stimulator cells. Supernatants were harvested after 18 hours and analyzed by cytometric bead array using the Bio-Plex Human Cytokine 17-Plex Panel (Bio-Rad Laboratories) according to the manufacturer's instructions.

Xenograft Models

All mouse experiments were approved by the COH Institute Animal Care and Use Committee. Six- to ten-week old NOD/*Scid* IL-2RγC^{null} (NSG) mice were injected intravenously (i.v.) on day 0 with 2×10^7 freshly thawed T cell products, either with or

without 2×10^7 irradiated (8,000 rads) NS0-IL15 cells given i.p. three times a week to provide a systemic supply of human IL-15 *in vivo,* as previously described [9]. Human T cell engraftment was determined by flow cytometric analysis of harvested tissues.

qPCR for WPRE copy number

Genomic DNA (gDNA) was prepared from frozen aliquots of the final product formulation of each qualification run using the QIAamp DNA Mini Kit (Qiagen) and then tested for the detection of WPRE DNA by quantitative polymerase chain reaction (qPCR) - primers and PCR conditions available upon request. To estimate the average number of genomic copies of integrated vector per cell, standard curves for WPRE copy numbers were established from serial dilutions of epHIV7 plasmid DNA (10 – 100,000 copies) using primers specific for WPRE sequence. Cell number standard curves were established from serial dilutions of a control plasmid containing the human albumin open reading frame [14] using primers specific for this endogenous cellular gene (2 alleles per cell). Clonal T cell lines with Southern blot verified WPRE integration copy numbers of one (cJ05585) and two (cF06011) were used to confirm the accuracy of this qPCR assay.

RCL assay

Frozen aliquots of the final product formulation (10^7 cells) from each qualification run were sent to Indiana University School of Medicine Vector Production Facility for replication competent lentivirus (RCL) testing using an assay modeled on guidelines recommended by the FDA for detecting replication competent retrovirus. Briefly, test samples were each used to inoculate a separate culture of C8166-45 cells (derived from human umbilical cord blood lymphocytes), which are permissive for infection and growth of HIV-1. The C8166-45 cells were then cultured for a minimum of 21 days to allow amplification of RCL. The indicator phase was carried out by infecting naïve C8166-45 cells with cell-free media from the amplification phase and passaging the cells an additional 7 days. At the end of the indicator phase, supernatants and genomic DNA were collected for p24 and psi-gag analysis, respectively. Analysis of supernatants for p24 was performed according to the HIV-1 p24 ELISA kit (Perkin Elmer) directions, and samples were required to contain p24 values below the limits of detection for the assay to be deemed RCL negative. Genomic DNA underwent PCR amplification followed by Southern blot analysis to detect psi-gag recombination sequences, and samples were required to have no evidence of psi-gag sequences to be deemed RCL negative.

Results

Performance of clinical scale CliniMACS immunomagnetic selection of human $CD8^+$ T_{CM}

We developed a two-step immunomagnetic process for selection of $CD8^+$ T_{CM} (Fig. 1) based on differential expression of the CD45RA (naïve versus memory T cells) and CD62L (central versus effector memory) surface markers. The first CliniMACS processing step achieves enrichment of $CD8^+CD45RO^+$ memory T cells by depletion of $CD45RA^+$ naïve T and B cells, $CD4^+$ T cells, and $CD14^+$ monocytes using Miltenyi GMP anti-CD45RA, -CD4, and -CD14 microbeads, respectively. The second CliniMACS processing run consists of a positive selection of $CD62L^+$ cells to eliminate $CD62L^-$ effector memory T cells by labeling with a combination of GMP anti-CD62L-biotin (biotinylated-DREG56 generated at COH) and Miltenyi anti-biotin microbeads. After magnetic depletion of 5×10^9 input PBMC, the percentage of naïve $CD45RA^+$ cells from five healthy donors was decreased from 81.2±1 to 10.2±2.8, the percentage of $CD4^+$ cells decreased from 55.6±3.8 to 2.4±0.9, and the percentage of $CD14^+$ monocytes decreased from 19.8±4.5 to 3±0.5 (Fig. 2A). Similar CliniMACS depletion results were generated in the processing of PBMC from two lymphoma donors (Fig. 2B). The mean cell yield in the target cell population following

depletion was 6.4±2.4 % of the input PBMC (Table 1). Subsequent CliniMACS™ positive selection of $CD62L^+$ T_{CM} cells using 0.1 μg biotinylated-DREG56 per 10^6 cells, a ratio based on competitive binding assays (Fig. S1A), resulted in enrichment of $CD62L^+$ lymphocytes from 23.9±5.3% to 70±3.9% (Fig. 2C). This flow cytometric evaluation, however, is most likely an underestimation of CD62L-positivity due to the competition between the PE-conjugated DREG56 mAb used for staining and the biotinylated-DREG56 mAb used in the magnetic selection process. To further define the resulting purity (Fig. S2) and yield (Table S1) of this two-step selection process we also performed 4-color flow cytometric analysis on three additional healthy donor PBMC both pre- and post-selection using a non-competing anti-CD62L mAb (SK11; Fig. S1B) and DAPI-defined exclusion of dead cells. This analysis revealed that, after selection, the non-T cell (i.e., CD8/CD3-negative) contaminants (25.1±17.4% of DAPI-negative cells) appeared to predominantly consist of $CD13^+$ myeloid cells (Fig. S2; i.e., cells which would not survive the IL-2/15-mediated expansion process to follow). As expected, the majority of T cells ($CD8^+$) were $CD45RO^+CD62L^{hi}$ T_{CM}, with a minor $CD45RO^+CD6L^{dim}$ population (Fig. S2). While we cannot rule out the potential contamination of T_{EM}, the similar expression levels of CCR7, CD27, CD28 and IL-7Rα on both the $CD45RO^+CD6L^{dim}$ and $CD45RO^+CD62L^{hi}$ cells is consistent with both populations being T_{CM}[15] and suggests that CD62L shedding may have occurred during the selection process[16]. Furthermore, analysis of CD45RA indicated that naïve T cells were not a contaminant (Fig. S2).

Following the second CliniMACS selection procedure, an average of 0.4±0.2% of the input PBMC were recovered (Tables 1 and S1). This is in contrast to the predicted average yield of 1.4±1.2%, as determined by the CD45RO, CD62L and CD8 expression profiles of the three additional healthy donor PBMC (Table S1). Together these data indicate that this CliniMACS immunomagnetic selection process produces a significantly enriched population of $CD62L^+$ T_{CM} with an approximate recovery efficiency of 26%.

Anti CD3/28 bead activation, lentiviral vector transduction and expansion of $CD8^+$ T_{CM}

To facilitate lentivirus transduction, $CD8^+$ T_{CM}-enriched cells were stimulated within 2 hrs after selection with Dynabeads® Human T expander CD3/CD28 in the presence rhIL-2 and rhIL-15. Three days later, these cultures were transduced with clinical grade CD19Rop-epHIV7 at MOIs ranging from 0 to 2.9 in Vuelife tissue culture bags (Table 2). The cells were then propagated in the Vuelife tissue culture bags with X Vivo15 media containing 10% FCS, and supplemented with rhIL-2 and rhIL-15 three times a week. Cell density was maintained at approximately 0.5×10^6/mL, and the growth kinetics for each of seven cell products indicated that exponential growth occurred over 3 to 4 weeks after the transduction (Fig. 3A). We observed that from a starting population of $7–15\times10^6$ transduced $CD8^+$ T_{CM}, derived from either healthy or lymphoma patient donors, cultures expanded to approximately 3×10^9 cells (600-fold) within 3–6 weeks without further stimulation (Fig. 3A). Thus, this process yields clinically relevant numbers of transduced $CD8^+$ $T_{E/CM}$ in a timely manner for clinical use.

To further evaluate the cytokine dependence of transduced $CD8^+$ $T_{E/CM}$ after their expansion and cryopreservation when they would be intended for patient infusion, cell products were thawed and washed, cultured in media alone or with cytokines (rhIL-2 and rhIL-15), and monitored for cell viability and growth (Fig. 3B). As expected, the continued viability of cells derived from both healthy donors and lymphoma patients was IL-2/IL-15 dependent and similar to the mock transduced product. Furthermore, after 28 days of cytokine-driven proliferation, withdrawal of rhuIL-2 and rhuIL-15 (i.e., with UCPIN 007, 008, 050 and 091), revealed the continued dependence of these cells on cytokine.

Cellular composition, vector copy number, and CAR expression of cryopreserved products

The purity of cell products after expansion to $>2\times10^9$ cells was assessed by flow cytometry for surface expression of TCRα/β, CD3, CD4, CD8 and CD14. We found that 97–99% of cells expressed CD3, and the majority of these T cells expressed TCRα/β (81–94%) and were $CD4^-CD8^+$ (97–99%) (Table 3). Lentivirus vector integration was evaluated by quantitative polymerase chain reaction (qPCR) specific for the vector's modified ORF-null WPRE sequence. The accuracy of this qPCR assay was qualified by quantifying the calculated WPRE copy number of clonal T cell lines with known WPRE integration sites of one (cJ05585) and two (cF06011) as determined by Southern analysis. Based on results from this analysis, the average number of WPRE copies per cell for the six products that were transduced ranged from 1.5–4.3 (Table 4). There was a positive correlation between MOI used for transduction and the detected average vector copy number per cell (R^2=0.6, P=0.03) (Fig. S3).

The amount of CAR expression and frequency of CAR expressing T cells derived from experiments in which T cells were transduced with lentivirus at different MOIs were analyzed in Western blots probed with anti-human CD3ζ and by flow cytometry with anti-human IgG4 Fc antibody (Fig. 4). Western blot analyses of each qualification run product confirmed expression of the 67-kDa CD19-specific CAR in each transduced product. Band quantitation of both the chimeric and the endogenous CD3ζ revealed that the ratio of CAR to endogenous ζ ranged from 0.6 to 1.2 at MOIs of 1.5 to 2.0, and the three production runs performed at a fixed MOI of 1.5 resulted in similar CAR:endogenous ζ ratio values of 0.7, 0.7 and 0.6 (Fig. 4A). Flow cytometry using the Fc-specific antibody to detect the CD19R revealed detectable cell surface CAR in 58–90% of transduced cells. At the MOI of 1.5, Fc^+ cells accounted for 58%, 70%, and 76% of cells (Fig. 4B). Based on these data, at an MOI of 1.5, reproducible CAR expression was obtained in the majority of T cells with an average vector copy number/cell value well below 5.0 - a threshold below which is recommended for clinical applications with genetically manipulated T cell products.

Cytolytic potency and effector cytokine secretion by $CD19R^+CD8^+$ $T_{E/CM}$ products

Quiescent $CD8^+$ T_{CM} cells express lower levels of effector molecules such as perforin and granzyme B than quiescent T_{EM}, but once differentiated to T_E cells, they acquire potent cytolytic activity triggered either through the CTL's endogenous TCR or through the CAR. To compare the total cytolytic potency of each cell product with that triggered by the CD19-specific CAR, we performed 4-hr chromium release assays using $CD19^+$ lymphoblastoid cell line (LCL) expressing a cell surface anti-CD3 scFv (LCL-OKT3) capable of activating all T cells through the CD3 complex, $CD19^+$ targets (LCL, SupB15) and $CD19^-$ K562 targets. Results from these assays confirmed that at the end of culture, cell products exhibit cytolytic activity, and that CAR triggered cytolysis was close to the maximal cytolytic output of cells when triggered by universal LCL-OKT3 target cells (Fig. 5A). Interestingly, the high level of CAR redirected cytolytic activity did not appear to correlate with the MOI used to transduce the cells (ranging from 1.5 to 2.9) or the differences in CAR expression between products. Of note, the product isolated from lymphoma patient UCPIN 108 exhibited low levels of cytolytic potency against LCL-OKT3 targets and $CD19^+$ targets. The etiology of this defect cannot be attributed to the cellular composition of this product that is similar to the other six production runs. Further studies are ongoing to determine if global signaling defects are present in this patient's T cells.

A second function of $CD8^+$ CTL is the synthesis and secretion of effector cytokines such as IFN-γ. Overnight stimulation of thawed $CD19R^+$ $CD8^+$ $T_{E/CM}$ with $CD19^+$ LCL or Sup-B15 cells, induced IFN-γ levels in culture supernatants in excess of 10 ng/ml in 6 of the 7

products (Fig. 5B). UCPIN 108 failed to secrete appreciable levels of IFN-γ in response to both LCL-OKT3 as well as $CD19^+$ stimulators, suggesting that the deficit observed in cytolysis is global in scope and intrinsic to the T cells from this patient (Fig. 5B). Overall polyfunctionality of the 7 cell products is also evidenced by CD19-specific induction of GM-CSF, IL-2 and/or TNF-α levels in the culture supernatants (Fig. 5C). Together these data demonstrate that transduction with CD19Rop-epHIV7 at an MOI as low as 1.5 yields cell products that exhibit CD19-specific CAR redirected cytolytic activity and cytokine production.

$CD19R^+CD8^+$ $T_{E/CM}$ products retain expression of CD62L, CD27, and CD28 and are polyclonal

Cell products exhibiting CAR redirected anti-tumor reactivity and lymph node homing would be desired for lymphoma immunotherapy. Consistent with our prior experience with propagating T_{CM} in vitro, wherein progressive loss of T_{CM} markers (CD62L, CCR7, CD28) occurred after repeated rounds of in vitro activation [8,9], the T_{CM}-derived cell products generated using a single CD3/CD28 Dynal bead activation contain significant numbers (30–40%) of $CD8^+$ T cells that retain CD62L, CD27, and CD28, both from healthy donors and lymphoma patients (Fig. 6A). Thus, while we can't discount the potential inclusion of contaminating T_{EM} (Fig. S2) in the final cell products, they are obviously significantly enriched for T_{CM}. Additionally, the cell products derived with this platform did not exhibit upregulation of PD-1 expression (Fig.6A). To verify that the phenotypic and functional attributes of cell products could be attributed to a general feature of T cells manufactured under this process rather than a spurious observation resulting from the disproportionate outgrowth of limited T cell clones in some products, we performed TCR Vβ analysis to assess polyclonality of the products. We found that T cell products from both healthy donors and lymphoma patients were polyclonal and had representation by all Vβ families (Fig. 6B). Thus, the acquisition of effector function and the retention of lymph node homing receptors in the polyclonal products are expected to be a reproducible feature of this manufacturing platform for deriving T cells for clinical trials.

In vivo engraftment of $CD19R^+CD8^+$ $T_{E/CM}$ products

We have developed an NSG mouse model for human T cell engraftment wherein T_{CM}-derived but not T_{EM}-derived $CD8^+$ T cells can engraft in a huIL-15 dependent manner [9]. The engraftment fitness assessment of cell products was examined three weeks following adoptive transfer (Day +24), a time point when transferred T_{EM}-derived effector cells would not be detectable by flow cytometric quantitation of human $CD45^+/CD8^+$ human T cells in bone marrow[9]. Detectable levels of T cell engraftment was observed in each individual NSG mouse receiving IL-15 support (Fig. 7A). This IL-15-dependent human T cell engraftment was observed with each cell product derived from both healthy donors (Fig. 7B) and lymphoma donors (Fig. 7C).

$CD19R^+CD8^+$ $T_{E/CM}$ products are RCL negative

As part of a safety assessment, frozen aliquots of the final product formulation from each qualification run were sent to Indiana University School of Medicine Vector Production Facility for replication competent lentivirus (RCL) testing as described in the methods. Test results for the presence of RCL in each of the seven qualification run samples were negative, based on both HIV-1 p24 ELISA and psi-gag PCR assays.

$CD19R^+CD8^+$ $T_{E/CM}$ products generated for current phase I/II clinical trial

In our current Phase I/II trial (IND #14645), we have used this same platform to successfully manufacture over 2×10^9 CD19-specific $CD8^+$ T_{CM}-enriched cell products from three

lymphoma patients, each within 28–33 days (Fig. 8A). Following transduction with clinical grade CD19Rop-epHIV7 lentivirus at an MOI of 1.5, these cell products, UCPIN 043, UCPIN 047 and UCPIN 048, were found to be 65.1%, 46.2% and 67.3% CAR^+ by Fc-specific staining, respectively (Fig. 8B), and exhibited CAR-mediated cytolysis (Fig. 8C). Both UCPIN 043 and UCPIN 048 displayed CD19-specific cytolytic activity similar to the maximal lysis triggered by LCL-OKT3 target cells; while CD19-specific cytolysis of UCPIN 047 was not as robust as that mediated by OKT3, possibly correlating with its lower CAR expression (Fig. 8C). Together these results further support the feasibility of using this manufacturing platform to produce potent CD19-specific $T_{E/CM}$ products from lymphoma patients in a manner that can be applied to clinical use.

Discussion

T cell products that are engineered to be specific for CD19 have broad application for adoptive therapy of B-lineage malignancies, and can potentially eliminate minimal residual disease that persists after conventional chemotherapy. Here we describe a semi-closed manufacturing process for reproducibly generating genetically modified CD19-specific T cells from a defined population of $CD8^+$ T_{CM} in a short period of time for clinical applications. The T cell products generated from our qualification runs express the CD19-specific CAR, and display CD19-mediated cytolytic function and cytokine production. Importantly, lentivirus transduction using a MOI of 1.5 provided maximal transduction efficiency, and increasing the MOI resulted in a higher number of integrated vector copies per cell but did not improve transduction efficiency. Broad TCR Vβ usage was observed in all cell products, suggesting that cell selection, transduction and expansion did not result in a T cell pool with a skewed TCR repertoire. The CD19-specific T cells retain expression of CD62L, CD27 and CD28, which have been associated with improved engraftment, and upon transfer into NSG mice, engraft *in vivo* in a huIL-15 dependent manner. Thus, while we can't rule out the potential inclusion of contaminating T_{EM} (Fig. S2) – though of similar phenotype to the $CD45RO^+CD62L^{hi}$ T_{CM} in every examined aspect besides CD62L levels - the final cell products are significantly enriched for T_{CM}.

The engraftment fitness of the T cell products described here may help address a barrier that has been observed in various clinical studies, where the safety and feasibility of cloned [17,18] and bulk [19,20] T cells has been established, but durable antitumor effects have not been achieved due to lack of T cell engraftment and/or persistence. Clinical experience with adoptive transfer of virus-specific T cells has revealed that only a subset of the infused cells can be detected long term in vivo [21]. Furthermore, in the melanoma trials of Rosenberg et al, where T cell engraftment is seen in 50% of patients, engraftment is often restricted to a subset of the infused T cells [22]. Findings such as these highlight the difficulty in predicting and/or generating uniform T cell products that can persist after adoptive transfer.

Efforts to prospectively identify T cell populations that exhibit superior capacity to engraft and/or persist after adoptive therapy have focused on analyzing subsets of virus specific T cells [8,23]. Indeed, Epstein Barr virus (EBV)-specific T cells engineered to co-express tumor-specific receptors survived longer in neuroblastoma patients than those lacking virus specificity, and were associated with tumor regression or necrosis in half of the subjects tested [24]. Studies in macaque and xenograft mouse models of adoptive T cell transfer have shown that virus-specific $CD8^+$ T cells derived from T_{CM} persist long-term *in vivo*, reacquire phenotypic and functional properties of memory T cells and occupy memory T cell niches [8,9]. Even the recent trials that have administered polyclonal effector T cells for the treatment of CLL and ALL have suggested that the gene-engineered cells detected long-term in patients have characteristics of T_{CM} [19,20]. Restifo et al have also defined a long-lived human memory T cell population that has been termed "memory stem cells", and has

an enhanced capacity for self-renewal and to give rise to T_{CM}, T_{EM} and T_E cells [25]. Compared with T_{CM} and T_{EM}, these lymphocytes have increased proliferative capacity, more efficiently reconstitute immunodeficient mice, and mediate superior in vivo antitumor responses [25,26].

At this time, it has yet to be determined whether a more uniform T-cell product as described here provides improved and/or more reproducible therapeutic benefit compared to that observed with 'conventional' bulk T cells. However, while the 'absolute best' T cell population for use in adoptive therapy will require prospective analysis in clinical trials, the capacity to engraft is a key property that correlates with therapeutic efficacy. It is likely that factors other than the (cell of origin will also play a role in the persistence of transferred cells in vivo and therapeutic efficacy. The recent clinical trial by Carl June et al, where non-selected CAR^+ T cells engrafted and mediated potent antitumor activity in patients with chronic lymphocytic leukemia [20,27], brings to light many of the key questions in the field. As alluded to above, was engraftment observed in this trial because some T_{CM} cells were transduced to express the CAR, and proliferated in vivo to mediate the delayed antitumor effects that were observed? Was the culture platform that utilized a single anti CD3/CD28 bead stimulation and short culture time key to the engraftment fitness of these cells? Indeed, it has been suggested that terminal differentiation of T_E cells during long-term culture – and the associated shortening of telomere length [28]- is responsible for the poor survival of transferred T cells observed in past clinical trials [29,30]. Alternatively, the 4-1BB costimulatory signaling domain present in the CAR or costimulatory ligands (CD80/86) expressed on CLL may have rescued transduced T cells from terminal differentiation. These issues will need to be resolved in future clinical trials, and can be best addressed if T cells of defined origin are utilized to derive the gene-modified T cell products.

Our platform for manufacturing CD19-specific $CD8^+$ T_{CM} is currently being applied to a Phase I/II COH held IND (#14645) for the treatment of high-risk intermediate grade B-lineage non-Hodgkin lymphomas. After a single stimulation with Dynal anti-CD3/CD28 beads followed by transduction with the CD19-specific scFvFc:ζ CAR containing lentiviral vector, and expansion in low dose IL-2/IL15, these cells are being infused within 3 days of HSCT while research participants are profoundly lymphopenic (i.e., after myeloablative chemotherapy/radiation). The Phase I portion of the study will evaluate the safety of this therapy and identify the maximum tolerated dose (MTD) of gene modified $CD8^+$ T_{CM} cells based on dose limiting toxicities (DLTs) while describing the full toxicity profile. The starting dose will be 50M, where $M = 10^6$. Dosing will escalate up to a maximum of 1000M, or until a dose limiting toxicity (DLT) is seen. The Phase II portion of the study aims to treat 12–15 research participants at the MTD and evaluate the rate of engraftment and persistence of the gene-modified T_{CM} cells *in vivo*.

Overall, we believe this strategy for enriching T_{CM}, followed by their lentitransduction and expansion provides a platform that may evolve to include other vectors and/or CAR to treat a wide variety of cancers/diseases. Based on our published work[8,9], we hypothesize that such T_{CM}-derived cell products can, upon encountering antigen-expressing tumor cells in vivo, successfully differentiate to effectors and provide therapeutic efficacy. Besides the selection of defined T cells for transduction, it is likely that conditioning of the host [31,32], inclusion of costimulatory domains in the tumor targeting receptors, and providing essential cytokines may further improve persistence and efficacy of tumor-specific T cells. At that juncture, it is likely that strategies will be needed to ablate the transferred cells to avoid prolonged toxicity to normal tissues (e.g., to allow the eventual outgrowth of normal B cells), or to regulate unwanted activity/proliferation of the engrafted T cells. Inducible suicide genes such as the herpes simplex virus thymidine kinase (HSV-TK) have been introduced into donor T cells to allow for ganciclovir-mediated prevention of graft versus

host disease. However, HSV-TK is foreign, and immune responses to HSV-TK expressing T cells have been found to lead to their premature elimination [18,33]. Another suicide strategy based on CD20 expression and the use of Rituximab has been developed [34–37], but this system would itself ablate B cells and is not compatible with T cell transfer in patients who are receiving Rituximab as part of the lymphoma/leukemia therapy. The inducible caspase 9 (iCasp9) suicide system, in which apoptosis of gene-modified cells is activated by an otherwise inert small-molecule dimerizer, has also gained recent interest after a single dose of the dimerizing drug was reported to ablate GVHD [38,39]. We have demonstrated the potential utility of a truncated EGFR (huEGFRt) expressed by transduced T cells for in vivo cell ablation following systemic cetuximab (Erbitux™) administration[40]. This huEGFRt is thus being incorporated into the vector of our next planned IND application to the FDA as a safety feature.

Supplementary Material

Refer to Web version on PubMed Central for supplementary material.

Acknowledgments

Source of Funding: This work was funded by NIH grants P50 CA107399, P01 CA030206, R01 CA136551, M01 RR0004, the Lymphoma Research Foundation, the Tim Nesvig Lymphoma Research Foundation, and the Marcus Foundation.

References

1. Dalgleish A, Pandha H. Tumor antigens as surrogate markers and targets for therapy and vaccines. Adv Cancer Res. 2007; 96:175–190. [PubMed: 17161680]
2. Drake CG, Jaffee E, Pardoll DM. Mechanisms of immune evasion by tumors. Adv Immunol. 2006; 90:51–81. [PubMed: 16730261]
3. Dudley ME, Rosenberg SA. Adoptive-cell-transfer therapy for the treatment of patients with cancer. Nat Rev Cancer. 2003; 3:666–675. [PubMed: 12951585]
4. Dudley ME, Wunderlich JR, Yang JC, et al. Adoptive cell transfer therapy following non-myeloablative but lymphodepleting chemotherapy for the treatment of patients with refractory metastatic melanoma. J Clin Oncol. 2005; 23:2346–2357. [PubMed: 15800326]
5. Dudley ME, Rosenberg SA. Adoptive cell transfer therapy. Semin Oncol. 2007; 34:524–531. [PubMed: 18083376]
6. Morgan RA, Dudley ME, Rosenberg SA. Adoptive cell therapy: genetic modification to redirect effector cell specificity. Cancer J. 2010; 16:336–341. [PubMed: 20693844]
7. Sadelain M, Brentjens R, Riviere I. The promise and potential pitfalls of chimeric antigen receptors. Curr Opin Immunol. 2009; 21:215–223. [PubMed: 19327974]
8. Berger C, Jensen MC, Lansdorp PM, et al. Adoptive transfer of effector CD8 T cells derived from central memory cells establishes persistent T cell memory in primates. J Clin Invest. 2008; 118:294–305. [PubMed: 18060041]
9. Wang X, Berger C, Wong CW, et al. Engraftment of human central memory-derived effector CD8+ T cells in immunodeficient mice. Blood. 2011; 117:1888–1898. [PubMed: 21123821]
10. Cooper LJ, Topp MS, Serrano LM, et al. T-cell clones can be rendered specific for CD19: toward the selective augmentation of the graft-versus-B-lineage leukemia effect. Blood. 2003; 101:1637–1644. [PubMed: 12393484]
11. Pelloquin F, Lamelin JP, Lenoir GM. Human B lymphocytes immortalization by Epstein-Barr virus in the presence of cyclosporin A. In Vitro Cell Dev Biol. 1986; 22:689–694. [PubMed: 3023278]
12. Gonzalez S, Naranjo A, Serrano LM, et al. Genetic engineering of cytolytic T lymphocytes for adoptive T-cell therapy of neuroblastoma. Journal of Gene Medicine. 2004; 6:704–711. [PubMed: 15170741]

13. Stastny MJ, Brown CE, Ruel C, et al. Medulloblastomas expressing IL13Ralpha2 are targets for IL13-zetakine+ cytolytic T cells. J Pediatr Hematol Oncol. 2007; 29:669–677. [PubMed: 17921847]
14. Charrier S, Stockholm D, Seye K, et al. A lentiviral vector encoding the human Wiskott-Aldrich syndrome protein corrects immune and cytoskeletal defects in WASP knockout mice. Gene Ther. 2005; 12:597–606. [PubMed: 15616597]
15. Sallusto F, Geginat J, Lanzavecchia A. Central memory and effector memory T cell subsets: function, generation, and maintenance. Annu Rev Immunol. 2004; 22:745–763. [PubMed: 15032595]
16. Smalley DM, Ley K. L-selectin: mechanisms and physiological significance of ectodomain cleavage. J Cell Mol Med. 2005; 9:255–266. [PubMed: 15963248]
17. Park JR, Digiusto DL, Slovak M, et al. Adoptive transfer of chimeric antigen receptor re-directed cytolytic T lymphocyte clones in patients with neuroblastoma. Mol Ther. 2007; 15:825–833. [PubMed: 17299405]
18. Jensen MC, Popplewell L, Cooper LJ, et al. Antitransgene rejection responses contribute to attenuated persistence of adoptively transferred CD20/CD19-specific chimeric antigen receptor redirected T cells in humans. Biol Blood Marrow Transplant. 2010; 16:1245–1256. [PubMed: 20304086]
19. Brentjens RJ, Riviere I, Park JH, et al. Safety and persistence of adoptively transferred autologous CD19-targeted T cells in patients with relapsed or chemotherapy refractory B-cell leukemias. Blood. 2011; 118:4817–4828. [PubMed: 21849486]
20. Kalos M, Levine BL, Porter DL, et al. T cells with chimeric antigen receptors have potent antitumor effects and can establish memory in patients with advanced leukemia. Sci Transl Med. 2011; 3:95ra73.
21. Turtle CJ, Swanson HM, Fujii N, et al. A Distinct Subset of Self-Renewing Human Memory CD8(+) T Cells Survives Cytotoxic Chemotherapy. Immunity. 2009
22. Huang J, Khong HT, Dudley ME, et al. Survival, persistence, and progressive differentiation of adoptively transferred tumor-reactive T cells associated with tumor regression. J Immunother (1997). 2005; 28:258–267.
23. Savoldo B, Huls MH, Liu Z, et al. Autologous Epstein-Barr virus (EBV)-specific cytotoxic T cells for the treatment of persistent active EBV infection. Blood. 2002; 100:4059–4066. [PubMed: 12393655]
24. Pule MA, Savoldo B, Myers GD, et al. Virus-specific T cells engineered to coexpress tumor-specific receptors: persistence and antitumor activity in individuals with neuroblastoma. Nat Med. 2008; 14:1264–1270. [PubMed: 18978797]
25. Gattinoni L, Lugli E, Ji Y, et al. A human memory T cell subset with stem cell-like properties. Nat Med. 2011; 17:1290–1297. [PubMed: 21926977]
26. Klebanoff CA, Gattinoni L, Palmer DC, et al. Determinants of successful CD8+ T cell adoptive immunotherapy for large established tumors in mice. Clin Cancer Res. 2011
27. Porter DL, Levine BL, Kalos M, et al. Chimeric Antigen Receptor-Modified T Cells in Chronic Lymphoid Leukemia. N Engl J Med. 2011
28. Tran KQ, Zhou J, Durflinger KH, et al. Minimally cultured tumor-infiltrating lymphocytes display optimal characteristics for adoptive cell therapy. J Immunother. 2008; 31:742–751. [PubMed: 18779745]
29. Gattinoni L, Klebanoff CA, Palmer DC, et al. Acquisition of full effector function in vitro paradoxically impairs the in vivo antitumor efficacy of adoptively transferred CD8+ T cells. J Clin Invest. 2005; 115:1616–1626. [PubMed: 15931392]
30. Kaech SM, Wherry EJ. Heterogeneity and cell-fate decisions in effector and memory CD8+ T cell differentiation during viral infection. Immunity. 2007; 27:393–405. [PubMed: 17892848]
31. Gattinoni L, Finkelstein SE, Klebanoff CA, et al. Removal of homeostatic cytokine sinks by lymphodepletion enhances the efficacy of adoptively transferred tumor-specific CD8+ T cells. J Exp Med. 2005; 202:907–912. [PubMed: 16203864]

32. Dudley ME, Yang JC, Sherry R, et al. Adoptive cell therapy for patients with metastatic melanoma: evaluation of intensive myeloablative chemoradiation preparative regimens. J Clin Oncol. 2008; 26:5233–5239. [PubMed: 18809613]
33. Berger C, Flowers ME, Warren EH, et al. Analysis of transgene-specific immune responses that limit the in vivo persistence of adoptively transferred HSV-TK-modified donor T cells after allogeneic hematopoietic cell transplantation. Blood. 2006; 107:2294–2302. [PubMed: 16282341]
34. Griffioen M, van Egmond EH, Kester MG, et al. Retroviral transfer of human CD20 as a suicide gene for adoptive T-cell therapy. Haematologica. 2009; 94:1316–1320. [PubMed: 19734426]
35. Serafini M, Manganini M, Borleri G, et al. Characterization of CD20-transduced T lymphocytes as an alternative suicide gene therapy approach for the treatment of graft-versus-host disease. Hum Gene Ther. 2004; 15:63–76. [PubMed: 14965378]
36. van Meerten T, Claessen MJ, Hagenbeek A, et al. The CD20/alphaCD20 'suicide' system: novel vectors with improved safety and expression profiles and efficient elimination of CD20-transgenic T cells. Gene Ther. 2006; 13:789–797. [PubMed: 16421601]
37. Vogler I, Newrzela S, Hartmann S, et al. An improved bicistronic CD20/tCD34 vector for efficient purification and in vivo depletion of gene-modified T cells for adoptive immunotherapy. Mol Ther. 2010; 18:1330–1338. [PubMed: 20461062]
38. Tey SK, Dotti G, Rooney CM, et al. Inducible caspase 9 suicide gene to improve the safety of allodepleted T cells after haploidentical stem cell transplantation. Biol Blood Marrow Transplant. 2007; 13:913–924. [PubMed: 17640595]
39. Di Stasi A, Tey SK, Dotti G, et al. Inducible apoptosis as a safety switch for adoptive cell therapy. N Engl J Med. 2011; 365:1673–1683. [PubMed: 22047558]
40. Wang X, Chang WC, Wong CW, et al. A transgene-encoded cell surface polypeptide for selection, in vivo tracking, and ablation of engineered cells. Blood. 2011; 118:1255–1263. [PubMed: 21653320]

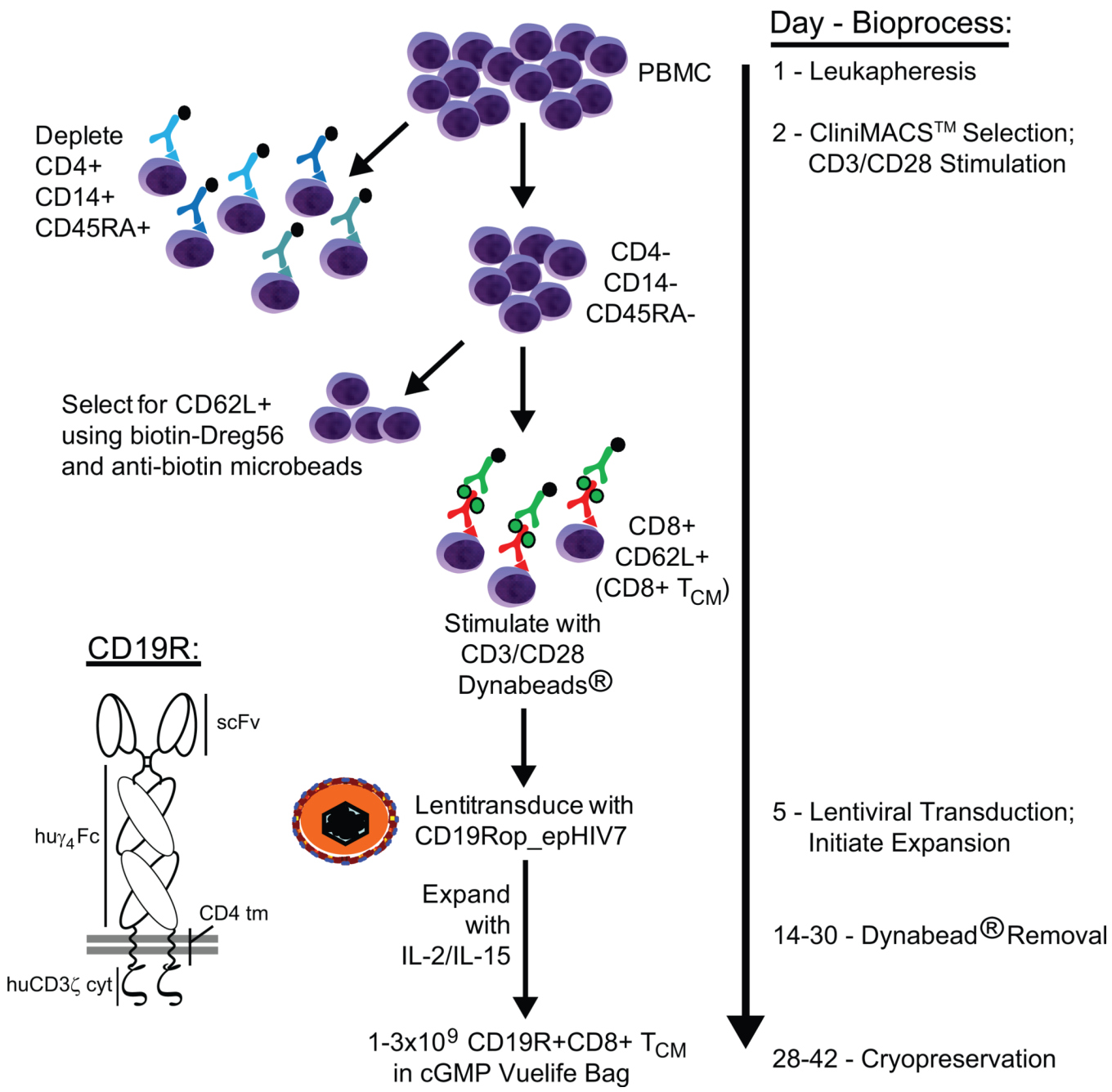

Figure 1. Process flow diagram for generation of CD19-specific CD8$^+$ T_{CM} cells under GMP guidelines

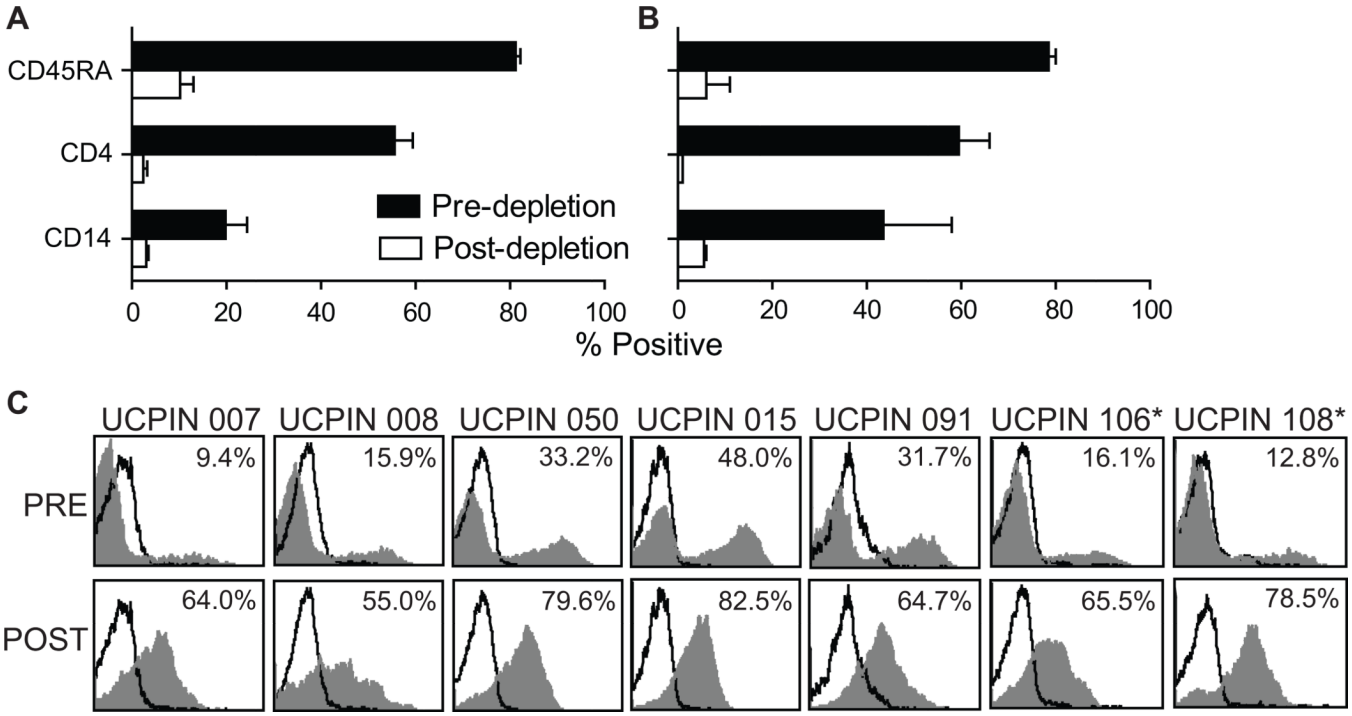

Figure 2. CliniMACS™ Selection of CD8$^+$ T_{CM}

PBMC from healthy donors (**A**, N=5) and lymphoma patients (**B**, N=2) were labeled with anti-CD45RA, anti-CD14, and anti-CD4 microbeads and underwent CliniMACS™ magnetic depletion. Percent cells expressing the naïve T cell marker CD45RA, the monocyte marker CD14, and the CD4 T cell marker pre- and post-depletion are depicted. **C**, After depletion, the CD45RA$^-$ CD14$^-$ CD4$^-$ cells were labeled with biotinylated anti-CD62L mAb (DREG56) followed by incubation with anti-biotin microbeads for selection of CD62L$^+$ cells on CliniMACS™. Percentage of CD62L+ (DREG56+) cells pre- and post-selection (grey histogram) was calculated using the subtraction method compared to staining with isotype control antibody (open histograms). *, UCPINs 106 and 108 were originally derived from lymphoma patient PBMC.

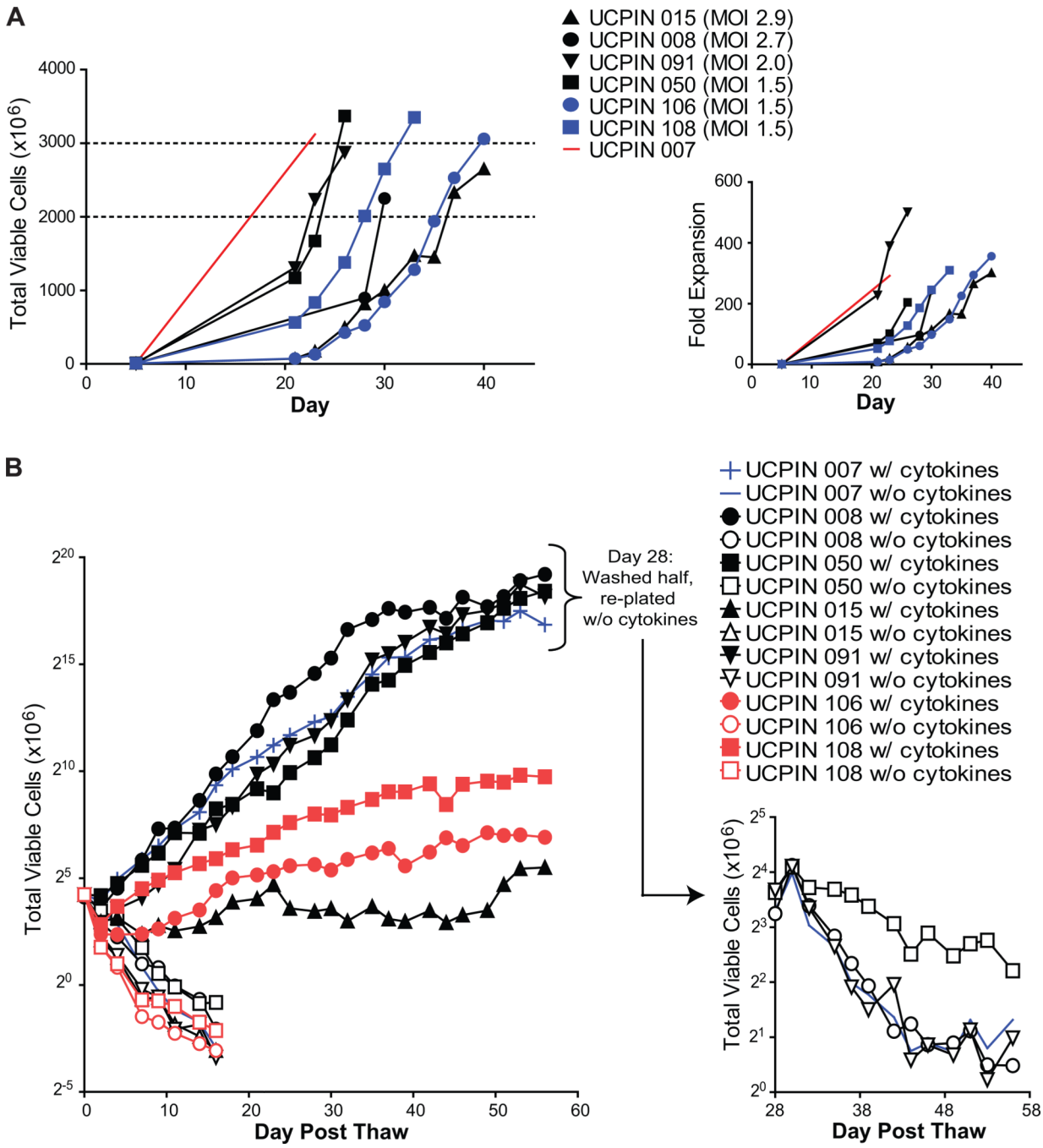

Figure 3. Expansion of gene-modified CD8+ T_{CM}-enriched products

A, Viable cell numbers starting at the day of magnetic enrichment +/− lentiviral transduction with CD19Rop-epHIV7 (day 5) are indicated for each cell product derived from healthy donors (red and black) and lymphoma patients (blue). Dashed lines demark the target cell number range of 2–3 × 10^9. Cryopreservation of each line occurred on the day of the last depicted data point. Right panel depicts fold expansion after magnetic enrichment of these same cell products. **B**, Freshly thawed nontransduced UCPIN 007 cells (blue) were compared to cell products that had been transduced with CD19Rop-epHIV7 for viable cell numbers upon culture with (filled symbols) or without (open symbols) rhuIL-2 and

rhuIL-15. Qualification run products that originated from lymphoma donor PBMC are indicated in red. To ensure cytokine dependence of UCPIN 007, 008, 050 and 091, half of these cells that had been cultured in with rhuIL-2 and rhuIL-15 were removed at day 28, washed, and re-plated for culture in the absence of cytokine prior to further monitoring of viable cell number (Right panel). Log 2 scales are depicted for the Y-axis to better depict doubling time of cells in culture.

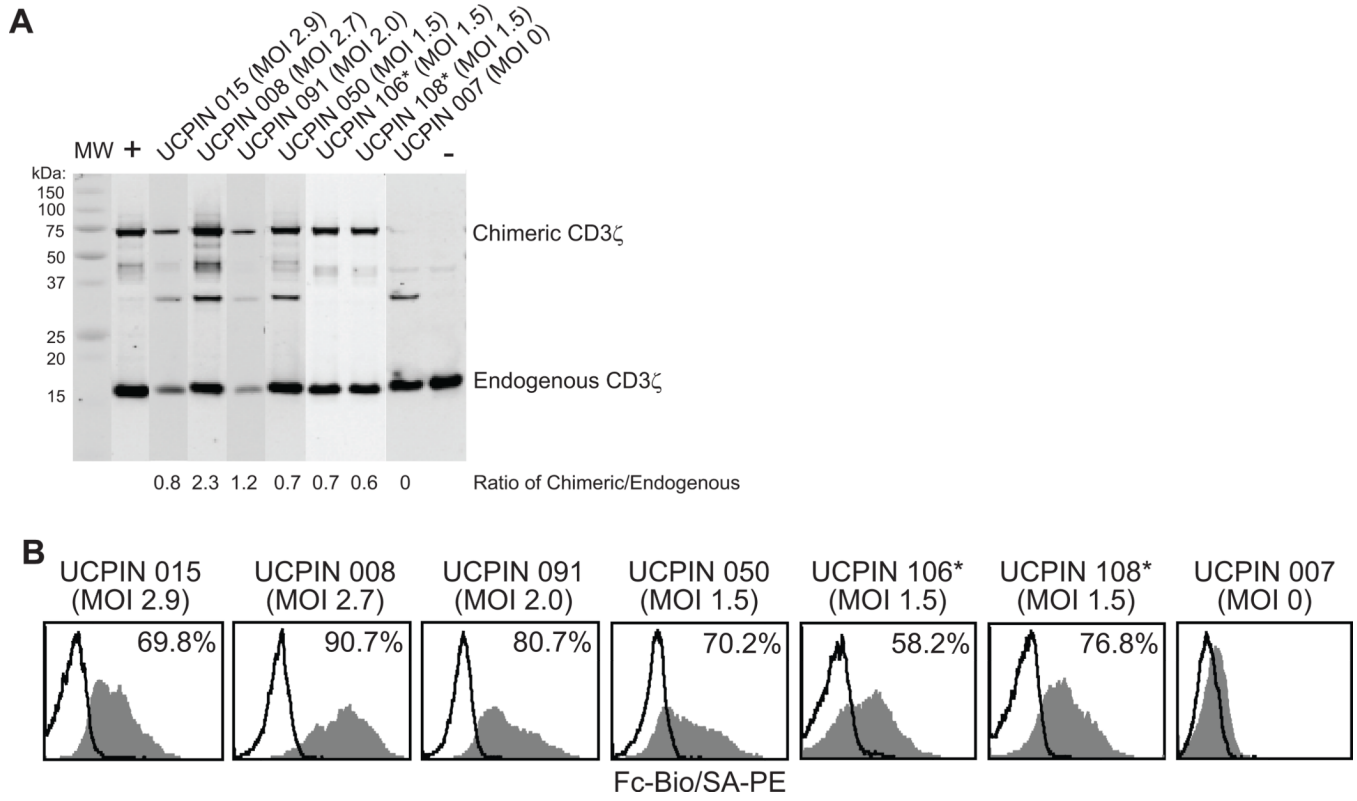

Figure 4. Expression of Fc-Containing Chimeric Receptor on gene modified CD8+ T_{CM}-enriched cells

CD8+ T_{CM} -enriched cells that were non-transduced (MOI 0) or transduced with CD19Rop-epHIV7, expanded to clinically relevant cell numbers and cryopreserved, were freshly thawed and examined by Western Immunoblot (**A**) and flow cytometry (**B**). **A**, Ratio of the band intensities for the 66-kDa ζ-containing CAR and 16-kDa endogenous ζ band for each cell product is depicted. **B**, Freshly thawed T cell products were stained with biotinylated anti-Fc antibody followed by PE-conjugated streptavidin (grey histogram) or SA-PE alone (open histograms). Percentage of immunoreactive cells was calculated using the subtraction method compared to staining of non-transduced UCPIN 007. *, UCPIN 106 and 108 were originally derived from lymphoma patient PBMC.

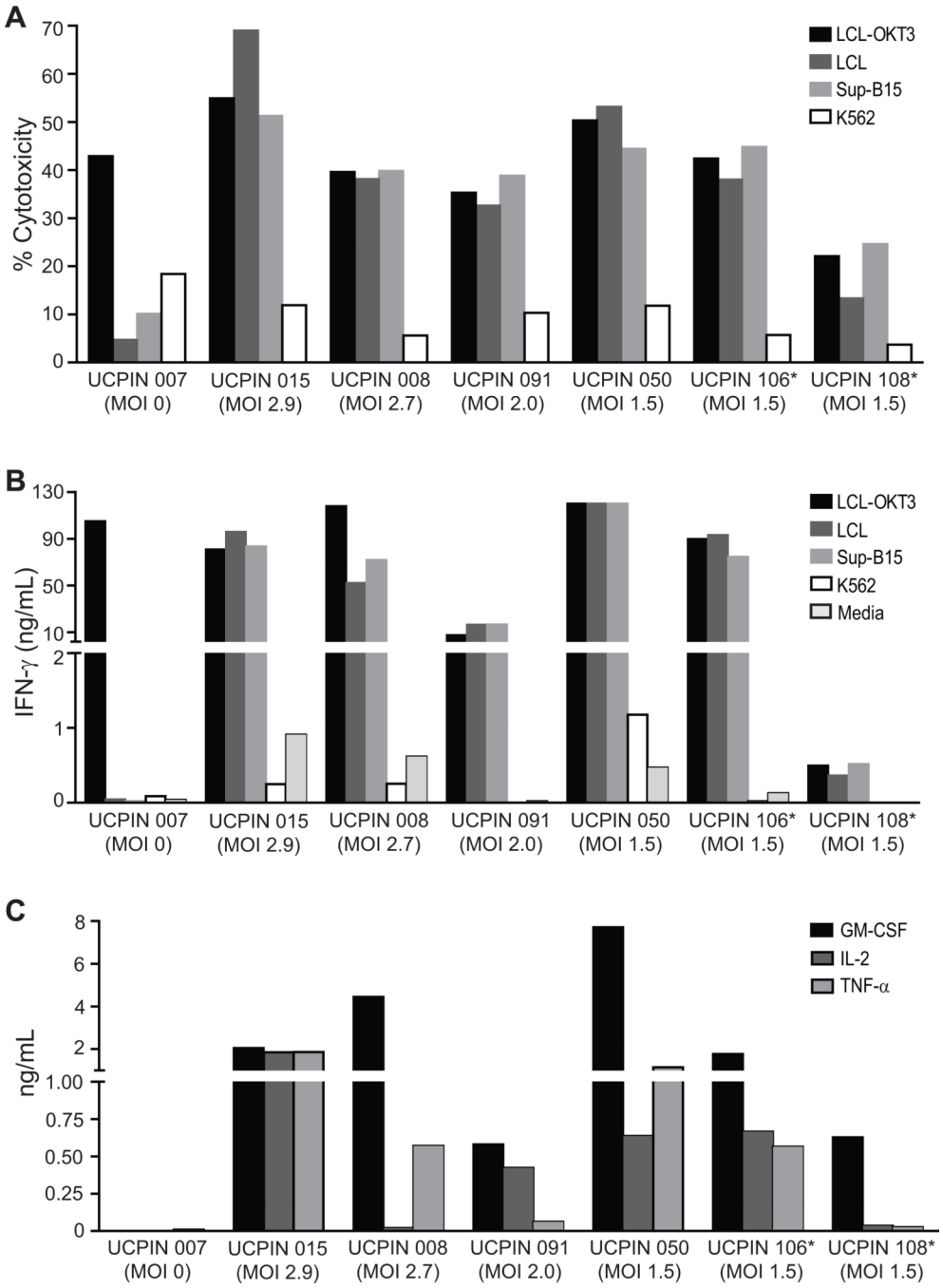

Figure 5. CD19-specific effector function of CD8+ T_{CM}-enriched CD19R$^+$ cells

A, ^{51}Cr-release assays were performed using freshly thawed T cell products as effectors against CD19-expressing targets LCL and SupB15, as well as LCL-OKT3 and K562 cells as positive and negative control targets, respectively. Cytolytic capacity at an E:T ratio 25:1 is depicted. **B**, Freshly thawed T cell products (10^5) from were co-cultured overnight in 96-well tissue culture plates with 10^5 of either CD19-expressing stimulators LCL and SupB15, or LCL-OKT3 and K562 cells as positive and negative control stimulators, respectively. Supernatants were harvested 18 hours after stimulation and IFN**γ** levels were analyzed by cytometric bead array. **C**, Freshly thawed T cell products were co-cultured with stimulators

as in **B**, and supernatants from co-cultures with SupB15 cells were analyzed for GM-CSF, IL-2 and TNF-α levels by cytometric bead array. *, UCPIN 106 and 108 were originally derived from lymphoma patient PBMC.

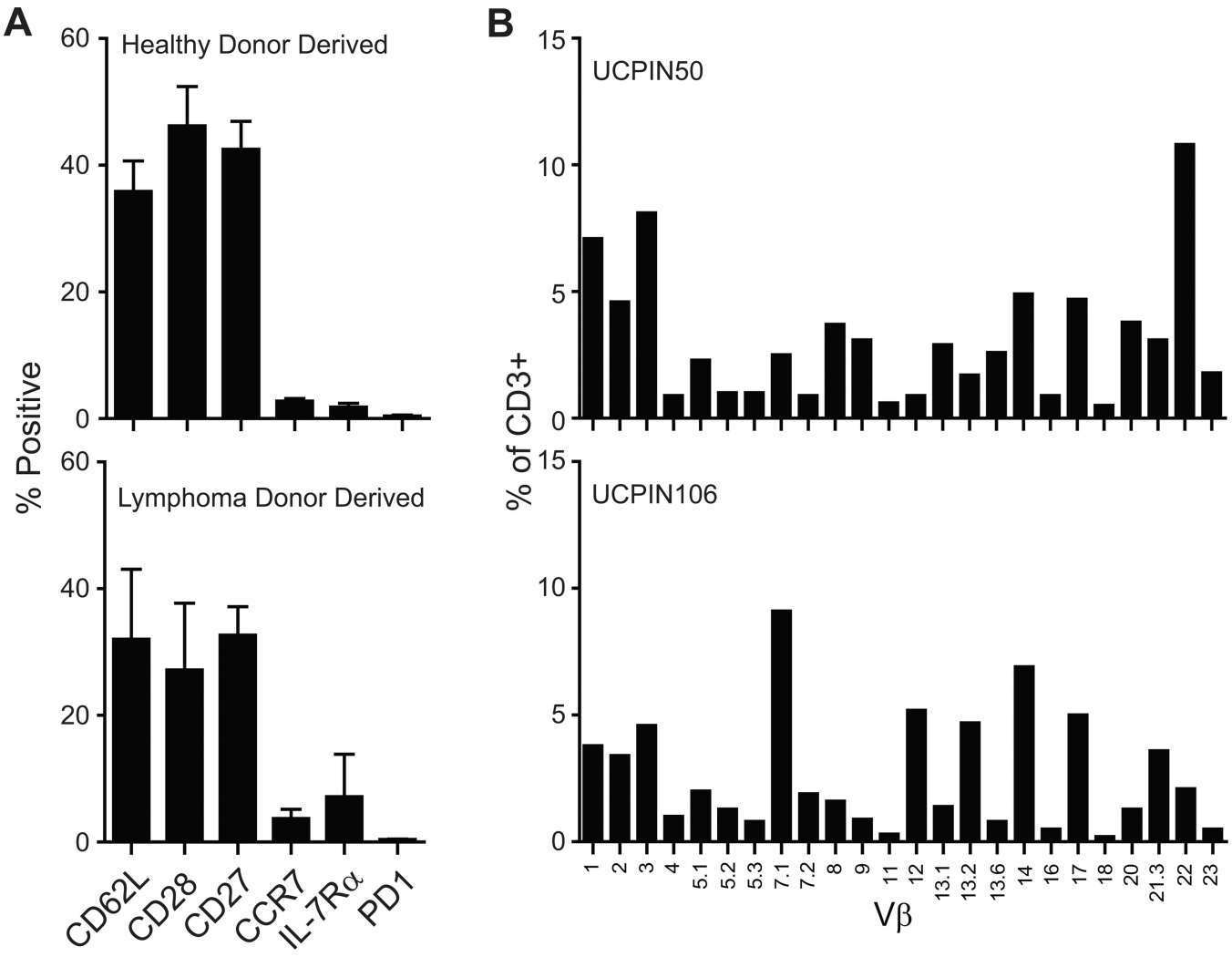

Figure 6. Extended surface phenotype of CD8+ T_{CM}-enriched CD19R$^+$ cells

A, Freshly thawed T cell products derived from healthy donors (top) and lymphoma patients (bottom) were examined for the mean expression (± S.E.) of CD62L, CD28, CD27, CCR7, IL-7Rα, and PD-1 by flow cytometry. **B,** Freshly thawed T cell products were stained with the IOTest® Beta Mark TCR V-beta Repertoire Kit an analyzed by flow cytometry. Percent of CD3$^+$ cells staining positive for the indicated Vβ genes on representative cell products from a healthy donor (UCPIN 050) and a lymphoma patient (UCPIN106) are depicted.

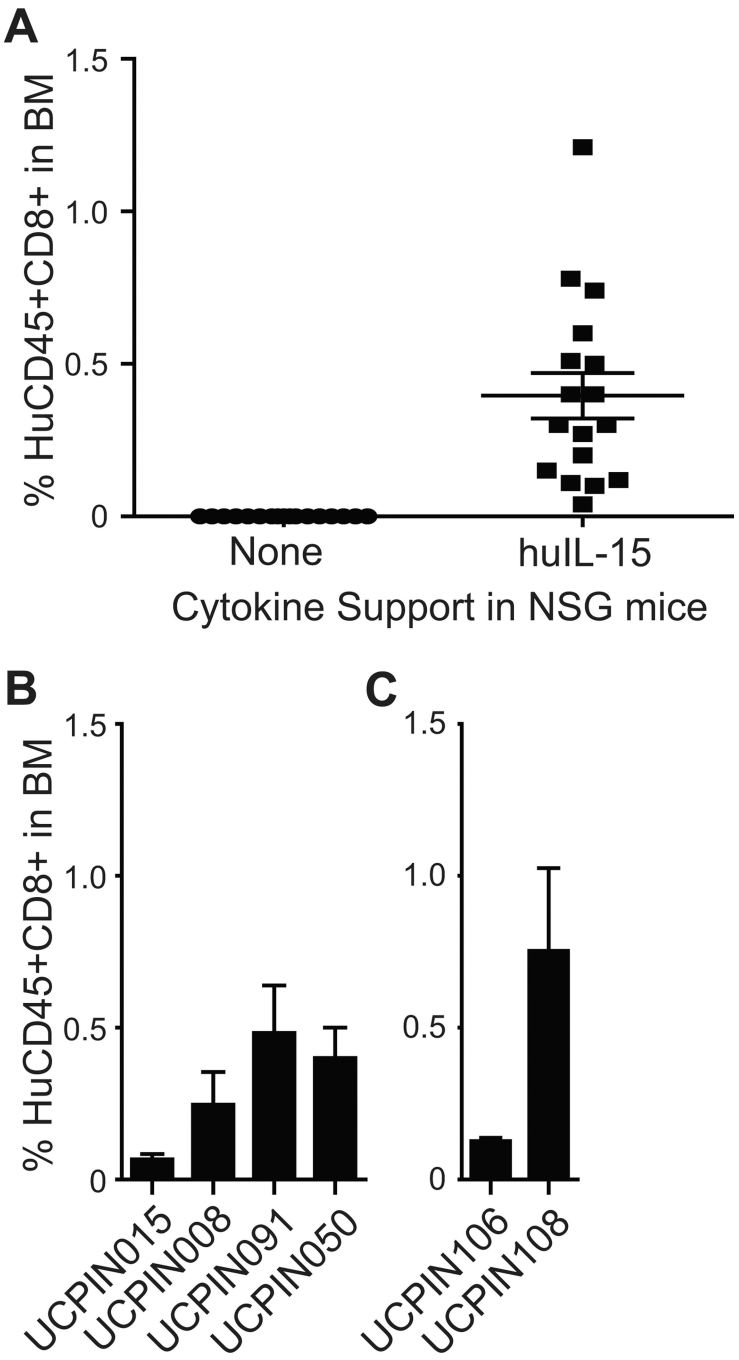

Figure 7. In vivo persistence of CD8+ T_{CM}-enriched CD19R$^+$ cells

10^7 T cells were infused i.v. into NSG mice either with or without irradiated NS0-IL15 cells i.p.; percent $CD45^+CD8^+$ human T cells in recipient mouse bone marrow was analyzed after 24 days by flow cytometry. **A**, Values from individual mice are depicted in the absence and presence of IL-15 support. **B** and **C**, Mean ± S.E. from n = 3 mice that received T cell products generated from either healthy donors (**B**) or lymphoma patients (**C**) in the presence of human IL-15.

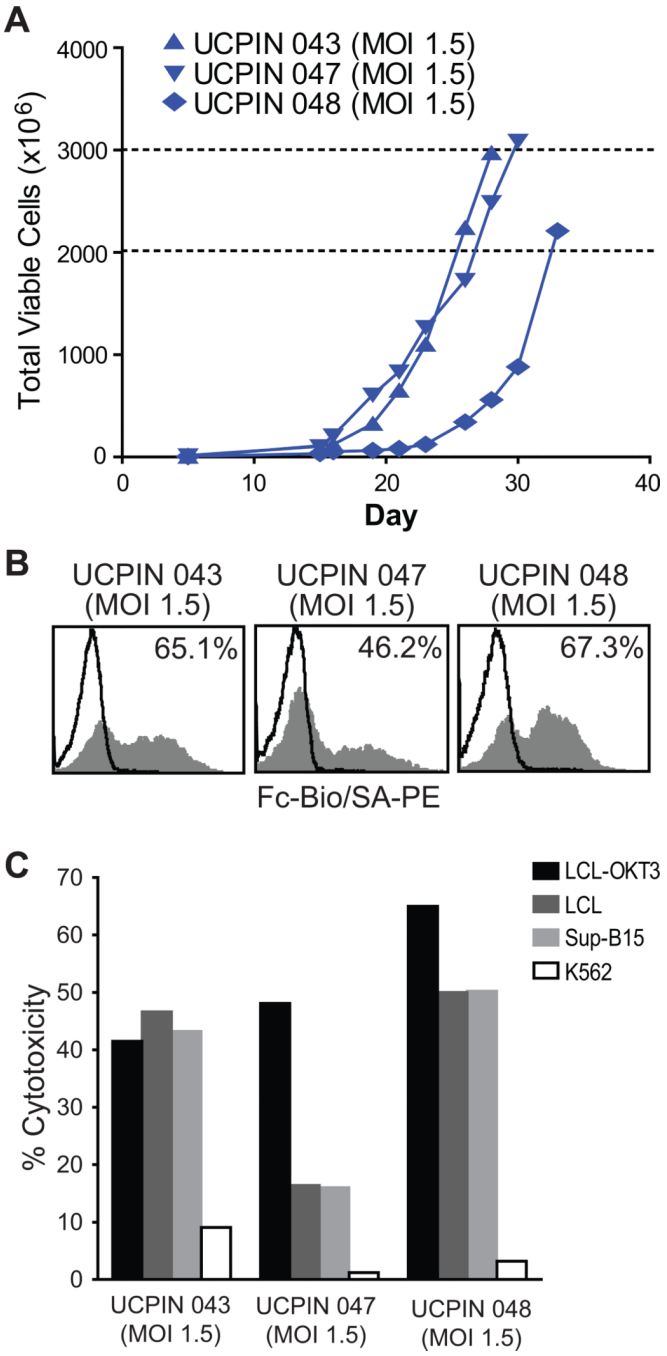

Figure 8. First two clinical products on current Phase I/II trial (IND #14645)

A, Viable cell numbers starting at the day of magnetic enrichment and lentiviral transduction with CD19Rop-epHIV7 (day 5) are indicated for each cell product derived from lymphoma patients enrolled on our current clinical trial. Dashed lines demark the target cell number range of 2–3 × 10^9. Cryopreservation of each line occurred on the day of the last depicted data point. **B**, Freshly thawed T cell products from lymphoma patients enrolled on our current clinical trial were stained with biotinylated anti-Fc antibody followed by PE-conjugated streptavidin (grey histogram) or SA-PE alone (open histograms). Percentage of immunoreactive cells was calculated using the subtraction method compared to staining with

SA-PE alone. **C,** ^{51}Cr-release assays were performed using freshly thawed T cell products as effectors against CD19-expressing targets LCL and SupB15, as well as LCL-OKT3 and K562 cells as positive and negative control targets, respectively. Cytolytic capacity at an E:T ratio 25:1 is depicted.

Table 1

Cell recovery from immunomagnetic $CD8^+$ T_{CM} process

Product #	Input PBMC ($\times 10^6$)	Negative fraction post CD4/14/45RA depletion ($\times 10^6$)	Positive fraction post CD62L selection ($\times 10^6$)
UCPIN 007	5000	509	20.4
UCPIN 008	4000	359	21.3
UCPIN 050	5000	316	35.9
UCPIN 015	5000	175	21.2
UCPIN 091	5000	260	9.3
UCPIN 106 *	3800	163	12.2
UCPIN 108 *	5000	312	14.4
Mean % ± SD	**100%**	**6.4 ± 2.4%**	**0.4 ± 0.2%**

* Product derived from lymphoma patient PBMC

Table 2

Manufacturing overview of gene-modified cell products.

Product # /Leukapheresis Date	PBMC Source	Cell Number Stimulated Day 2 ($\times 10^6$)	Cell Number Transduced Day 5 ($\times 10^6$)	Multiplicity of Infection (MOI)
UCPIN 007/030410	Healthy Donor	20.4	10.7	0
UCPIN 008/022510	Healthy Donor	21.3	9.2	2.7
UCPIN 050/031110	Healthy Donor	35.9	16.5	1.5
UCPIN 015/031810	Healthy Donor	21.2	8.8	2.9
UCPIN 091/040110	Healthy Donor	9.3	5.7	2.0
UCPIN 106/040810	Lymphoma Donor	12.2	8.6	1.5
UCPIN 108/042210	Lymphoma Donor	14.4	10.8	1.5

Table 3

Surface phenotype of gene-modified cell products.

Product #	%TCRα/β+	%CD3+	%CD4+	%CD8+	%CD14+
UCPIN 007	87.2	97.3	0.9	98.0	14.2
UCPIN 008	88.9	99.1	1.4	98.0	0.6
UCPIN 050	92.5	96.9	2.7	97.5	6.6
UCPIN 015	94.9	98.8	0.2	98.8	0.0
UCPIN 091	94.1	99.4	0.8	99.1	1.2
UCPIN 106	85.2	97.9	3.2	98.3	N.D. *
UCPIN 108	81.4	99.3	1.5	97.0	N.D.

*N.D., Not done

Table 4

Vector copy number of manufactured cell products

Product #	MOI	Average Copies/Cell (S.D.)
cJ05585 (known single copy control)	NA	0.9 (0.0)
cF06011 (known two copy control)	NA	1.9 (0.4)
UCPIN 015	2.9	3.0 (0.3)
UCPIN 008	2.7	4.3 (2.1)
UCPIN 091	2.0	1.5 (0.4)
UCPIN 050	1.5	1.9 (0.5)
UCPIN 106 *	1.5	3.2 (0.9)
UCPIN 108 *	1.5	2.6 (0.7)
UCPIN 007	0	0.0 (0.0)

* Product derived from lymphoma patient PBMC